

# Alabama In Huntsville

## NAGW 996: 1993-1994 Annual Progress Report

In the past year, we have made considerable progress in a number of areas including algorithm development, completion of two major case studies, and the development of a new EUV flux model. As a result, there have been a major improvement in our ability to model global emissions in support of NASA's imaging plans. Five papers are currently in press. One of these was written by an undergraduate student.

### 1. HIGHLIGHTS

- Developed a new algorithm to allow physical models to reproduce observed  $NmF2$ .
- Investigated the relationship between  $NmF2$  and F10.7 at Millstone Hill during 1990.
- Developed a new solar EUV flux model.
- Statistical survey of anomalously high nighttime electron  $T_e$  at Millstone Hill.
- Conducted a case study of the March 1990 magnetic storm.
- Conducted a comparison between theory and data of magnetically quiet behavior of the winter ionosphere at Millstone Hill.

### 2. DESCRIPTION

The ability to accurately model F-region electron densities is extremely important in all aspects of ionospheric modeling. Our FLIP model has proved capable of reproducing the measured daytime densities very well using a technique that we developed to eliminate uncertainties due to neutral winds [Richards, 1991]. However, in common with other models, the nighttime densities are generally about a factor of 3 smaller than the observed densities.

There are many applications for which the electron density is just an ancillary input to the calculation to some other quantity to be studied, for example, when calculating emission rates or electron temperatures. These applications require very accurate electron densities. Empirical models such as the IRI model reproduce the average measured  $NmF2$  and  $hmF2$  very well but are unable to produce day-to-day variability the way a physical model can. Also, the topside density profiles are poorly modeled mainly because the topside is poorly sampled and more variable.

We have developed a new technique which allows the FLIP model to reproduce the measured  $NmF2$  as well as the measured  $hmF2$  (or an empirical model  $NmF2$  and  $hmF2$ ). The FLIP model then fills in the topside ionosphere self-consistently. Thus the accuracy of all those densities, temperatures, and emissions that depend on electron density has been greatly improved. The contour plot in Figure 1 demonstrates the new capability of the FLIP model to reproduce the observed electron density. A paper on this new technique is in preparation. The IRI model has been modified to make it a callable routine that returns just  $NmF2$  and  $hmF2$  so that they can be used in the FLIP model when measured  $NmF2$  and  $hmF2$  are not available. As a result, the FLIP model now has the capability of reproducing the IRI  $NmF2$  and  $hmF2$  while producing more physically realistic topside densities. The FLIP model is run in the normal mode without  $NmF2$

(NASA-CR-195781) [ACCURATE  
MODELING OF F-REGION ELECTRON  
DENSITIES] Annual Progress Report,  
1993-1994 (Alabama Univ.) 8 p

N94-30014

Unclass

normalization when studying how well the current theory allows the model to reproduce the electron density data, while in those studies that demand accurate electron densities as ancillary information, the  $NmF2$  normalization is invoked.

As mentioned in our previous annual report, a study of the ionosphere at solar maximum was conducted with the original intention of ascertaining the effects of vibrationally excited  $N_2$  ( $N_2^*$ ) on F-region ion densities because our previous studies indicated that vibrationally excited  $N_2$  should be important in summer at solar maximum but not in winter. We performed comparisons between our FLIP model and a large amount of Millstone Hill digisonde and Hobart ionosonde data for 1990 when the solar activity was generally very high but also varied by a factor of 2. We found that the measured densities were almost insensitive to solar activity while the model had a linear dependence on solar activity. When vibrationally excited  $N_2$  was included in the calculation, the model and data were brought into agreement.

Further investigation in the past 6 months revealed inadequacies in our EUV flux model as well as in other commonly used solar EUV flux models. As a result of a detailed study of available EUV flux data, a new solar extreme ultraviolet flux model, based on the F74113 reference spectrum and the AE-E relative flux measured variations, has been developed and a paper is now in press. The new EUV flux model (EUVAC) produces 50-575 Å fluxes that are in excellent agreement with the most reliable measurements (Figure 2). The photoelectron fluxes produced using EUVAC are also in excellent agreement with measured photoelectron fluxes. The variation of the fluxes with daily F10.7 from EUVAC is smaller than the fluxes from the older model. This is because the long term average F10.7 flux was constant even though the daily F10.7 index changed a lot in 1990. With the development of the new EUV flux model there was excellent agreement between the modeled and measured  $NmF2$  at both Hobart and Millstone Hill in 1990 without the need to invoke  $N_2^*$ . The observed lack of variation in  $NmF2$  as a function of daily F10.7 is partly due to the relationship between F10.7 and the solar EUV flux but is also due to changes in the thermosphere.  $N_2^*$  was not needed to produce good agreement between model and data under these conditions and further study will be needed to quantify its role in the ionosphere. This study has been reported in a paper that is in press.

An undergraduate student (Trevor Garner), has been doing research in regard to anomalous electron temperature enhancements over Millstone Hill. Trevor has done a detailed study of the occurrence characteristics of these events and found that it is mostly a winter phenomenon which occurs on 70% of the January nights and rarely in summer. However, it also occurs from September through May. The events typically occur prior to midnight and last for 2-3 hours. This behavior seems to rule out a direct link to conjugate photoelectron heating which should be absent at the equinoxes and present all night in January. He presented a poster paper on this subject at the 1992 CEDAR meeting and also at the NASA sponsored Magnetospheric Models conference held at Guntersville, Alabama in October 1993. A paper submitted to the Journal of Geophysical Research is in press. The newly developed capability of the FLIP model to reproduce measured  $NmF2$  and  $hmF2$  will be extremely useful in studying the mechanism that leads to the elevated temperatures at Millstone Hill. We will be able to determine the characteristics of the plasmaspheric heat flux that causes the enhanced temperatures. This could lead to a better understanding of plasmaspheric processes.

A major study has been conducted of the ionospheric behavior at Millstone Hill and Arecibo during the March 1990 magnetic storms. It was found that the FLIP model reproduced the electron density very well at Millstone Hill and at Arecibo during the quiet periods and during the first of two storms. During the second storm, which occurred two days after the first, the FLIP model was not capable of reproducing the measured electron density as well. These results have been presented at a special storm workshop at

Millstone Hill in March 1993, at the Baltimore AGU meeting in May 1993, and at the June 1993 CEDAR meeting in Boulder in 1993 and a journal paper is in preparation.

Another major study was conducted in conjunction with the Lower Thermosphere Coupling Study (LTCS). The FLIP model electron temperature and density were compared with the radar measurements at Millstone Hill in December 1989 and 1991. These periods were very quiet magnetically but the solar activity was high. The measured and modeled densities were very close during the day but the model nighttime densities were low by 50% to a factor of 2. When the  $NmF2$  normalization was used, the model temperature agreed very well with the measured temperature. These results were presented in a special session at the December 1993 AGU meeting in San Francisco. A paper is in preparation on this topic.

During 1993, a graduate student (Michael Zhu) developed the framework for a new empirical thermospheric wind model based on the techniques I have developed [Richards, 1991]. This work is being continued by Kevin Zou. The first version of the new wind model is on schedule to be completed by the end of summer 1994. Krishna Madakasiri is developing a new model of the peak height and density of the F2 region for use with the Richards [1991] technique for deriving winds from  $hmF2$ .

An ancillary task under this grant was to make the FLIP model available to the wider community by installing it at NCAR. This has been accomplished and it is now part of the official CEDAR data base of

models.

### 3. REFERENCES

- Feng, W., Ogawa, H. S., and D. L. Judge, The absolute solar soft X ray flux in the 20- to 100-Å region, *J. Geophys. Res.*, **94**, 9125, 1989.
- Hinteregger, H. E., K. Fukui, and B. R. Gilson, Observational, reference and model data on solar EUV, from measurements on AE-E, *Geophys. Res. Lett.*, **8**, 1147, 1981.
- P. G. Richards, An improved algorithm for determining neutral winds from the height of the F2 peak electron density, *J. Geophys. Res.*, **96**, 17893-17846, 1991.
- Tobiska, W. K., Revised solar extreme ultraviolet flux model, *J. Atmos. Terr. Phys.*, **53**, 1005, 1991.

### 4. PUBLICATIONS

1. "Ionospheric effects of the March 1990 magnetic storm: comparison of theory and measurement," P. G. Richards, D. G. Torr, M. J. Buonsanto, and D. P. Sipler, To be submitted to *J. Geophys. Res.*, **99**, May, 1994.
2. "Anomalous nighttime electron temperature events over Millstone Hill," T. W. Garner, P. G. Richards, R. H. Comfort, in press, *J. Geophys. Res.*, **99**, March, 1994.
3. "F2 peak electron density at Millstone Hill and Hobart: Comparison of theory and measurement at solar maximum," P. G. Richards, D. G. Torr, B. W. Reinisch, R. R. Gamache, and P. Wilkinson, in *J. Geophys. Res.*, **99**, March, 1994.

4. "EUVAC: A solar EUV flux model for aeronomic calculations" P. G. Richards, J. A. Fennelly, and D. G. Torr, in press, *J. Geophys. Res.*, 99, March, 1994.
5. "F2 peak electron density at solar maximum: Comparison of theory and measurement," P. G. Richards, D. G. Torr, B. W. Reinisch, and R. R. Gamache, in press. proceedings of the 7th International Ionospheric Effects symposium, March, 1993.
6. "New sources for the hot oxygen geocorona," P. G. Richards, M. P. Hickey, and D. G. Torr, in press, *Geophys. Res. Lett.*, April 1994.
7. "Objectives and preliminary results from the Imaging Spectrometric Observatory flown on ATLAS 1," D. G. Torr, M. R. Torr, M. F. Morgan, T. Chang, J. K. Owens, J. A. Fennelly, P. G. Richards, T. W. Baldrige, Submitted to *J. Geophys. Res.*, 97, April, 1994.
8. "Sensitivity of the 6300 Å twilight airglow from McDonald Observatory to neutral composition," D. J. Melendez-Alvira, D. G. Torr, P. G. Richards, W. R. Swift, M. R. Torr, and H. Rassoul. Submitted to *J. Geophys. Res.*, 98, August, 1993.
9. "Determination of ionospheric conductivities from FUV auroral emissions," G. Germany, P. G. Richards, D. G. Torr, and M. R. Torr, Submitted to *J. Geophys. Res.*, 99, February, 1994.
10. "Simultaneous retrieval of the solar EUV flux and neutral thermospheric O, O<sub>2</sub>, N<sub>2</sub>, and temperature from twilight airglow," Fennelly, J. A., D. G. Torr, P. G. Richards, and M. R. Torr, *J. Geophys. Res.*, 99, 6483, 1994.
11. "Thermospheric OI 844.6 nm emission in twilight," F. Bahsoun-Hamade, R. H. Wiens, G. G. Shepherd, and P. G. Richards, *J. Geophys. Res.*, 99, 6289, 1994.
12. "The use of FUV auroral emissions as diagnostic indicators," G. Germany, M. R. Torr, D. G. Torr, and P. G. Richards. Submitted to *J. Geophys. Res.*, 99, 383, 1994.
13. "Re-evaluation of the O<sup>+</sup>(<sup>2</sup>P) quenching rate coefficients using Atmosphere Explorer-C observations," Tsao Chang, D. G. Torr, P. G. Richards, and S. C. Solomon, *J. Geophys. Res.*, 98, 15589, 1993.

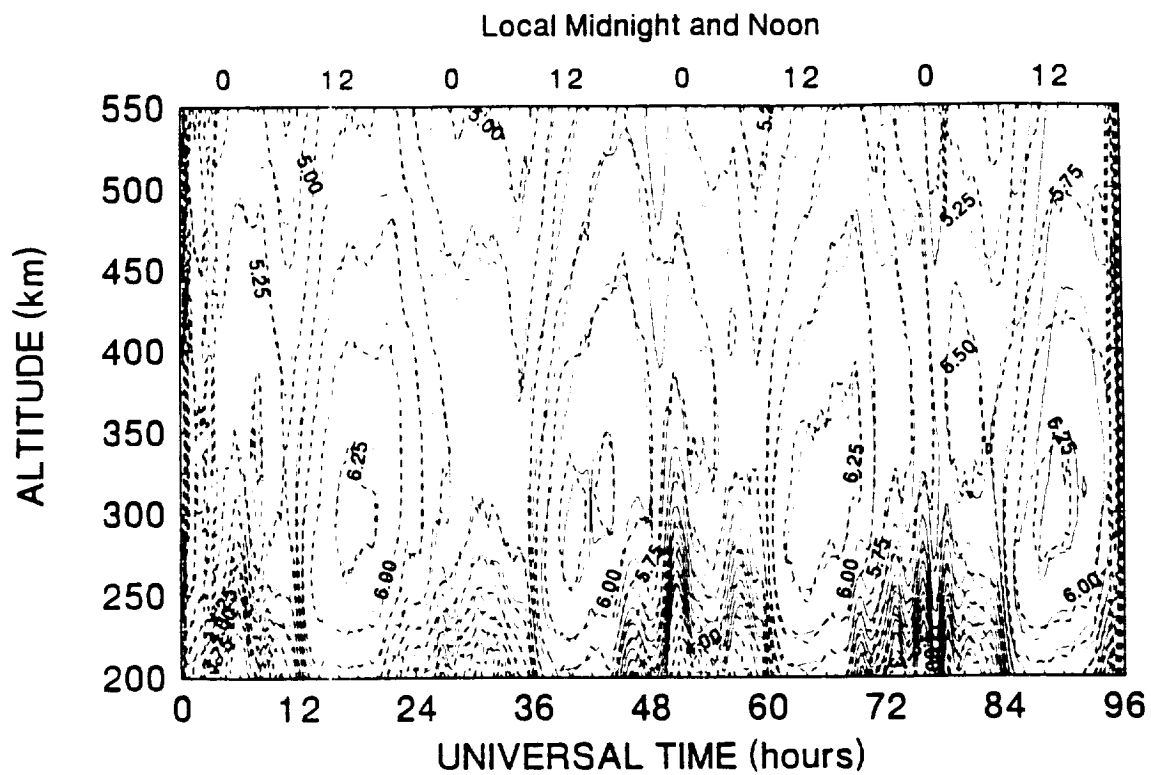


Figure 1: This figure shows the remarkably good agreement between the measured electron density (dashed contours) and the modeled electron density from the FLIP model using the new  $NmF2$  technique. The measurements were made at Millstone Hill from December 8 to 11, 1991

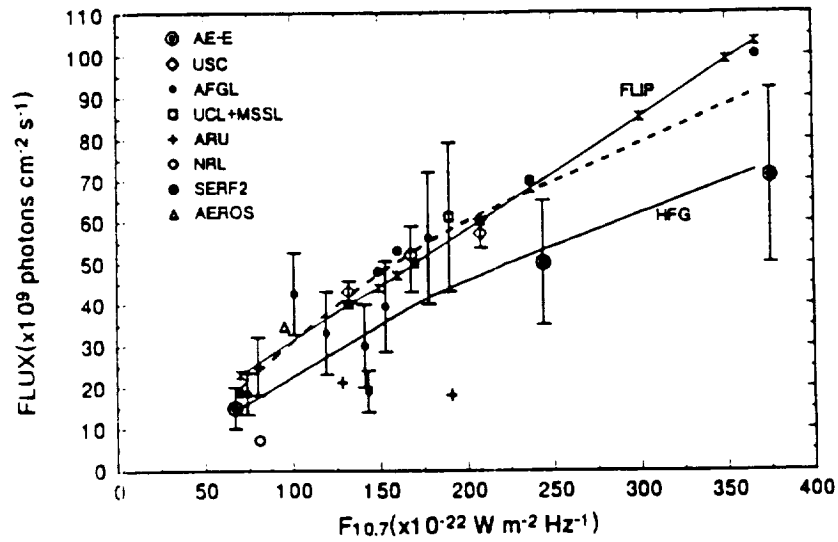


Figure 2: The measured total EUV 50-575 Å irradiance as a function of  $F_{10.7}$ . See *Feng et al.* [1989] for details of the measurements and *Tobiska* [1991] for SERF2 model values. Note that we have circled the AE-E fluxes given by Feng et al. to distinguish them from the AFGL rocket measurements. The solid line with asterisks is the integrated flux from the FLIP model. The solid line labeled HFG is a weighted least squares fit to the *Hinteregger et al.* [1981] model output for the AE-E measurement period between mid 1977 and the end of 1980. The broken curve is a weighted least squares fit to the output from our new model (EUVAC) for the same period.

# Reevaluation of the $O^+(^2P)$ Reaction Rate Coefficients Derived From Atmosphere Explorer C Observations

T. CHANG AND D. G. TORR

*Department of Physics/Center for Space Plasma and Aeronomic Research  
University of Alabama, Huntsville*

P. G. RICHARDS

*Computer Science Department/Center for Space Plasma and Aeronomic Research  
University of Alabama, Huntsville*

S. C. SOLOMON

*Laboratory for Atmospheric and Space Physics, University of Colorado, Boulder*

$O^+(^2P)$  is an important species for studies of the ionosphere and thermosphere: its emission at 7320 Å can be used as a diagnostic of the thermospheric atomic oxygen density. Unfortunately, there are no laboratory measurements of the O and  $N_2$  reaction rates which are needed to determine the major sinks of  $O^+(^2P)$ . The reaction rates that are generally used were determined from aeronomic data by Rusch et al. (1977) but there is evidence that several important inputs that they used should be changed. We have recalculated the O and  $N_2$  reaction rates for  $O^+(^2P)$  using recent improvements in the solar EUV flux, cross sections, and photoelectron fluxes. For the standard solar EUV flux, the new  $N_2$  reaction rate of  $3.4 \pm 1.5 \times 10^{-10} \text{ cm}^3 \text{ s}^{-1}$  is close to the value obtained by Rusch et al. (1977), but the new O reaction rate of  $4.0 \pm 1.9 \times 10^{-10} \text{ cm}^3 \text{ s}^{-1}$  is about 8 times larger. These new reaction rates are derived using neutral densities, electron density, and solar EUV fluxes measured by Atmosphere Explorer C in 1974 during solar minimum. The new theoretical emission rates are in good agreement with the data for the two orbits studied by Rusch et al. and they are in reasonable agreement with data from five additional orbits that are used in this study. We have also examined the effect of uncertainties in the solar EUV flux on the derived reaction rates and found that 15 % uncertainties in the solar flux could cause additional uncertainties of up to a factor of 1.5 in the O quenching rate.

## 1. INTRODUCTION

The 7320/7330 Å doublet arising from the transition  $O^+(^2D - ^2P)$  is a very important emission for studies of the thermosphere. For example, Fennelly et al. [1991] and McDade et al. [1991] have shown how ground-based twilight measurements of this feature can be used to retrieve altitude profiles of atomic oxygen. However, the accuracy of the retrieval depends on the validity of the photochemical model adopted for  $O^+(^2P)$ .

There are no laboratory measurements for key  $O^+(^2P)$  reaction rates and the rates that are currently used by the aeronomy community were derived from Atmosphere Explorer measurements by Rusch et al. [1977] using the best information that was available at that time. By combining the solar EUV fluxes and photoionization cross sections, they were able to deduce chemical reaction rates for losses of  $O^+(^2P)$  to atomic oxygen and molecular nitrogen. Over the past 15 years, there have been important refinements to some of the input parameters that were used by Rusch et al. [1977]. These refinements include changes to the solar EUV flux, photoionization cross sections, and the importance of photoelectron impact ionization. R. Link (private communication, 1990) pointed out the need to update the Rusch et al. model to take into account these refinements.

Problems with the solar EUV flux were discovered by Richards and Torr [1984] when they compared the measured shape of the photoelectron spectrum with the expected theoretical shape from the F74113 solar EUV flux spectrum of Hinteregger et al. [1977]. Another factor affecting the photoionization rate is the modification of the photoionization cross sections for O which are lower than those used in previous AE work. These new cross sections have been measured by Samson and Pareek [1985] and Angel and Samson [1988]. In the work of Rusch et al. [1977], ion production by photoelectron impact was thought to be small and neglected, but more recent work by Richards and Torr [1988] yielded significant production rates that ranged from 0.14 to 0.23 of the photoionization rate between the altitudes from 180 km to 350 km. The ratio is altitude dependent because it is a function of EUV attenuation, photoelectron transport, and whether or not the conjugate ionosphere is sunlit.

The objective of this paper is to reevaluate the reaction rate coefficients for  $O^+(^2P)$  with O and  $N_2$  in light of the new information on solar fluxes, cross sections, and photoelectron fluxes. Therefore we have reanalyzed the two orbits used by Rusch et al. [1977], and five additional AE-C orbits.

## 2. THEORY

$O^+(^2P)$  is produced in the ionosphere by photoionization and by photoelectron impact ionization of O. It is lost in reactions with neutrals and electrons and by radiation. The major source of  $O^+(^2P)$  is photoionization of O by wave-

Copyright 1993 by the American Geophysical Union.

Paper number 93JA00957.  
0148-0227/93/93JA-00957 \$05.00

## Use of FUV auroral emissions as diagnostic indicators

LEO J. BARNES, JAMES E. CRONIN, and G. B. DICKINSON

Department of Physics and Astronomy, University of Alabama in Huntsville, Huntsville, Alabama 35894

Received 15 May 1993; revised 15 September 1993; accepted 15 September 1993

Copyright © 1994 by John Wiley & Sons, Inc.

0893-9479/94/010383-06\$04.00

ABSTRACT

The FUV auroral emissions from the FUVIS instrument on the IMAGE spacecraft are used to

diagnose the auroral processes occurring during the IMAGE mission.

The FUVIS instrument is a wide-field-of-view, wide-bandwidth, FUV imager.

The FUVIS instrument is a wide-field-of-view, wide-bandwidth, FUV imager.

The FUVIS instrument is a wide-field-of-view, wide-bandwidth, FUV imager.

The FUVIS instrument is a wide-field-of-view, wide-bandwidth, FUV imager.

The FUVIS instrument is a wide-field-of-view, wide-bandwidth, FUV imager.

The FUVIS instrument is a wide-field-of-view, wide-bandwidth, FUV imager.

The FUVIS instrument is a wide-field-of-view, wide-bandwidth, FUV imager.

The FUVIS instrument is a wide-field-of-view, wide-bandwidth, FUV imager.

The FUVIS instrument is a wide-field-of-view, wide-bandwidth, FUV imager.

The FUVIS instrument is a wide-field-of-view, wide-bandwidth, FUV imager.

The FUVIS instrument is a wide-field-of-view, wide-bandwidth, FUV imager.

The FUVIS instrument is a wide-field-of-view, wide-bandwidth, FUV imager.

The FUVIS instrument is a wide-field-of-view, wide-bandwidth, FUV imager.

The FUVIS instrument is a wide-field-of-view, wide-bandwidth, FUV imager.

The FUVIS instrument is a wide-field-of-view, wide-bandwidth, FUV imager.

The FUVIS instrument is a wide-field-of-view, wide-bandwidth, FUV imager.

The FUVIS instrument is a wide-field-of-view, wide-bandwidth, FUV imager.

The FUVIS instrument is a wide-field-of-view, wide-bandwidth, FUV imager.

The FUVIS instrument is a wide-field-of-view, wide-bandwidth, FUV imager.

The FUVIS instrument is a wide-field-of-view, wide-bandwidth, FUV imager.

The FUVIS instrument is a wide-field-of-view, wide-bandwidth, FUV imager.

The FUVIS instrument is a wide-field-of-view, wide-bandwidth, FUV imager.

The FUVIS instrument is a wide-field-of-view, wide-bandwidth, FUV imager.

The FUVIS instrument is a wide-field-of-view, wide-bandwidth, FUV imager.

The FUVIS instrument is a wide-field-of-view, wide-bandwidth, FUV imager.

The FUVIS instrument is a wide-field-of-view, wide-bandwidth, FUV imager.

The FUVIS instrument is a wide-field-of-view, wide-bandwidth, FUV imager.

The FUVIS instrument is a wide-field-of-view, wide-bandwidth, FUV imager.

The FUVIS instrument is a wide-field-of-view, wide-bandwidth, FUV imager.

The FUVIS instrument is a wide-field-of-view, wide-bandwidth, FUV imager.

The FUVIS instrument is a wide-field-of-view, wide-bandwidth, FUV imager.

The FUVIS instrument is a wide-field-of-view, wide-bandwidth, FUV imager.

The FUVIS instrument is a wide-field-of-view, wide-bandwidth, FUV imager.

The FUVIS instrument is a wide-field-of-view, wide-bandwidth, FUV imager.

The FUVIS instrument is a wide-field-of-view, wide-bandwidth, FUV imager.

The FUVIS instrument is a wide-field-of-view, wide-bandwidth, FUV imager.

The FUVIS instrument is a wide-field-of-view, wide-bandwidth, FUV imager.

The FUVIS instrument is a wide-field-of-view, wide-bandwidth, FUV imager.

The FUVIS instrument is a wide-field-of-view, wide-bandwidth, FUV imager.

The FUVIS instrument is a wide-field-of-view, wide-bandwidth, FUV imager.

The FUVIS instrument is a wide-field-of-view, wide-bandwidth, FUV imager.

The FUVIS instrument is a wide-field-of-view, wide-bandwidth, FUV imager.

The FUVIS instrument is a wide-field-of-view, wide-bandwidth, FUV imager.